International Journal of Power Electronics and Drive Systems (IJPEDS)
Vol. 15, No. 4, December 2024, pp. 2660~2673
ISSN: 2088-8694, DOI: 10.11591/ijpeds.v15.i4.pp2660-2673

PV/T water-based cooling in hot climate conditions by using semi-circle baffles

Hayder Altharwanee, Francisco Jurado, David Vera
Department of Electrical Engineering, Faculty of Engineering, University of Jaén, Linares, Spain

Article Info

Article history:

Received Mar 21, 2024
Revised Aug 29, 2024
Accepted Sep 5, 2024

Keywords:

Nusselt number
Pressure drop
PV/T
SCB
Semi-circle baffles

ABSTRACT

PV/T water-based system using multi-row semi-circle baffles (SCB) is numerically investigated. Experimental validation was carried out in hot climate conditions. Factors associated with heat transfer enhancement, like Nusselt number, pressure drop, friction factor, electrical efficiency, and thermal efficiency, were calculated and discussed to show the impact of SCB on photovoltaic or PV cooling and system performance. Six different magnitudes of Reynolds number (500-4000), and mass flow rate (0.0137-0.0998) L/s at different radiation values were carried out in the simulation. Results indicated that utilizing SCB has an important effect on the PV/T system. In comparison to the smooth channel, the average Nusselt number of the enhanced channel increased by around (31.57-132.18)%, and the friction factor increased by (21.93-95.7) % while the thermal efficiency increased by about (16.34-79.29)%. These results indicate the system's good performance in terms of photovoltaic panel cooling and power production. PV surface temperature reduced by about (4-20) ℃. The electrical efficiency improved up to 32% and 49% for the smooth and enhanced channels respectively. The cost-benefit ratio (CBR) of the enhanced channel demonstrated that there is no detrimental influence of the pressure drop on the thermal performance.

Corresponding Author:

Francisco Jurado
Department of electrical engineering, Faculty of Engineering, University of Jaén
Andalucia, Linares, Spain
Email: fjurado@ujaen.es

NOMENCLATURE

A	: Collector surface area	G	: Radiation	γ	: C_p/C_v ratio
C_p	: Constant pressure heat capacity	m	: Mass flow rate	ρ	: Fluid density
L	: Channel length	k	: Thermal conductivity	ζ, CD_w	: Terms in SST model
Nu	: Nusselt number	h	: Convection heat transfer coef	η	: Thermal efficiency
Re	: Reynolds number	G	: Radiation	δ_{ij}	: Kronecker's delta
T_i, T_o	: Inlet and outlet temperature	S	: Surface area	μ	: Viscosity
T_w, T_b	: Wall and bulk temperature	S_{ij}	: Strain rate tensor	μ_T	: Turbulence viscosity
q	: Heat transfer rate	y	: Distance from the nearest wall	$a_1, \beta, \beta^*, \sigma_k, \sigma_\omega$	: Constants in SST model
ω	: Turbulence frequency	u_i, u_j	: Velocity vectors	τ_{ij}	: Stress tensor
f	: Friction factor	x_i, x_j	: Position vectors	μ	: Viscosity
P_k	: Production by shear	P	: Pressure	SST	: Shear stress transport
U	: Average velocity	T	: Temperature	SCB	: Semi-circle baffles
ΔP	: Pressure difference	F_1	: Blending function	CBR	: Cost-benefit ratio

1. INTRODUCTION

The world's demand for fossil energy caused increasing concentrations of emissions, or carbon dioxide (co_2), in the atmosphere layer, thus increasing the average global temperature. Carbon emissions are mostly caused by the excessive use of fossil fuels, garbage, and agricultural and industrial operations [1]. The Paris Agreement aims to reduce global warming to 1.5 °C by 2030, with zero emissions by 2050 [2]. To meet these goals, renewable energy must be used more extensively.

One of the most common methods for generating sustainable energy is through photovoltaic systems, which convert sunlight into electricity. This method can decrease emissions in industrial countries by 18% [3]. Despite high solar energy absorption, PV systems have poor efficiency (about 20% [4] or up to 30% in the best production cases [5]). Consequently, the remaining solar radiation is transformed into thermal energy [6]. Excessive heat causes a high surface temperature of the photovoltaic system and reduces its efficiency, so that a one-degree increase in photovoltaic temperature reduces electrical efficiency by (0.4–0.5)% [7]; additionally, overheating can damage all PV systems [8]; therefore, scientists and researchers tried and are still trying to solve this problem and enhance the PV performance.

The photovoltaic thermal (PVT) system concept was presented in 1976 [9], and this approach has developed over the decades until today. Many investigators and researchers are working on traditional PVT systems, while others are developing new approaches [10]. There are two strategies to improve the performance of PV systems and limit the negative effects of excessive panel surface temperatures: active, which requires external force, and passive, which does not require external force and is considered more efficient than the active way [11]. Passive methods include baffles [12], grooves [13], ribs [14], extended surfaces by using fins [15], twisted tape [16], porous [17], phase change material (PCM) [18], nanofluid [19], and vortex generator [20]. Passive approaches are a reliable and low-cost option for improving solar panel systems [21], so researchers have focused on developing this technology. With regard to baffles or vortex generators as a passive technique, numerous efforts have been made to improve the performance of solar systems. Vortex generation is a passive technique used in heat transfer and enhancement fields. Vortex generators force fluids to change direction, creating miniature vortices or eddies. These vortices can help break down the fluid's inactive boundary layer near the surface and weak regions, as well as increase heat transfer efficiency by speeding up the mixing process. Furthermore, the large drop in pressure near the vortex generators enhances the system's thermal performance.

However, the negative effects, such as flow restriction and cost, may be unintended consequences. Zhou and Ye [22] conducted experimental work on the thermal flow by utilizing curved trapezoidal vortex generators and found that increasing curvature and angle of inclination, along with a small attack angle, resulted in the optimum thermohydraulic performance. Kumar and Prasad [23] conducted a study on the thermal effects of using twisted tape in a solar water collector. According to their inquiry, the solar water collector achieved its best performance at a Reynolds number of 12000. Wang and Zhao [24] investigated the properties of heat flow by employing small-scale cylindrical baffles.

Their findings demonstrated a significant enhancement in heat transfer efficiency. Wijayanta *et al.* [25] conducted an experiment using a winglet vortex generator inserted into a circular tube to examine its impact on heat transfer. The improved tube demonstrated significantly higher thermal performance compared to the smooth tube at attack angles of 30°, 50°, and 70°, with performance factors ranging from 110% to 131%, 157% to 188%, and 218% to 264%, respectively. Maadi *et al.* [26] employed conical-leaf inserts within a cooling tube for the PV/T system in their research. The study participants discovered that the thermal efficiency was 14.1% when inserts were employed, however, it dropped to 10.2% when smooth tubes were utilized.

The study conducted by Zhou *et al.* [27] examined the role of a vortex generator in passive cooling of photovoltaic (PV) systems by free convection. The researchers discovered that the implementation of vortex generators resulted in a temperature reduction of approximately (2-3) ℃ in PV modules. Kaewchoothong *et al.* [28] studied the thermal performance of a PV/T employing various rib forms, and they noticed that a (V-shaped) rib gives the most efficient results. Previous investigations have addressed the thermal impact of using vortex generators with air as a working fluid. However, no study has explored the use of water as a working fluid in this context, particularly in hot climate conditions, Furthermore, there is no study with the same geometry design as this study. As a result, the present study investigates the thermal effect of using a multi-row of semi-circle baffles as vortex generators inside a rectangular channel to recover excess heat from PV systems. This work selected water as a coolant due to its superior thermal capacity over air [29].

2. WORK METHOD

The current work involves a numerical analysis to demonstrate the thermal performance of the PVT system. This is achieved by utilizing a series of the semi-circle baffles (SCB) within rectangular channels that are positioned on the rear sheet of the photovoltaic panel. The SCB, which is a vortex generator, is utilized to improve the thermal performance of the system, as stated recently. Numerical procedures which include geometry design, mesh, boundary conditions, grid independent, solution control and validation were carried on

using the principles of computational fluid dynamics (CFD). The results were validated by comparing them to the experimental test results. The following sections provide the experimental and numerical simulation details.

2.1. Experimental installation

The test platform was collected and set in Babil, Iraq (32 N, 44 E). In September 2022, the PV and PVT systems were set up at an inclination of 35°, directed towards the south, where a high ambient temperature was recorded. Figures 1(a) and 1(b) show an illustration diagram of the experimental setup. The system consists of a photovoltaic (PV) panel, a photovoltaic thermal collector PVT, a water tank, an inverter, a battery, a data logger, a water pump, and a flow meter. The PV/T collector comprises 14 copper channels affixed to the absorber plate. The PV back sheet ties and fixes to the smooth side of the absorber, while a glass wool layer insulates the other side. The PV/T materials and their descriptions are shown in Table 1. Recorded radiation values were (300, 470, 615, and 750) W/m^2, and the mass flow rate values were (0.0137, 0.0210, 0.037, 0.049, 0.074, and 0.0998) kg/s. The inlet water temperature was 27.15 °C, the ambient temperature ranged from (40 to 46) °C, and the wind speed was 3 m/s. In this study, temperature sensors PT100 and k-type were employed to measure temperature with an accuracy of 1%. The temperature was collected using a data recorder (TK-7Y) with an accuracy of 2%. The fluid flow was regulated using a flow meter K100, which has a measure range of (0.2 to 2) l/min and an accuracy of +-2.5 %. The site www.tutiempo.net was used to acquire radiation magnitude data. The experimental work's goal is to validate the numerical solution to the proposed study.

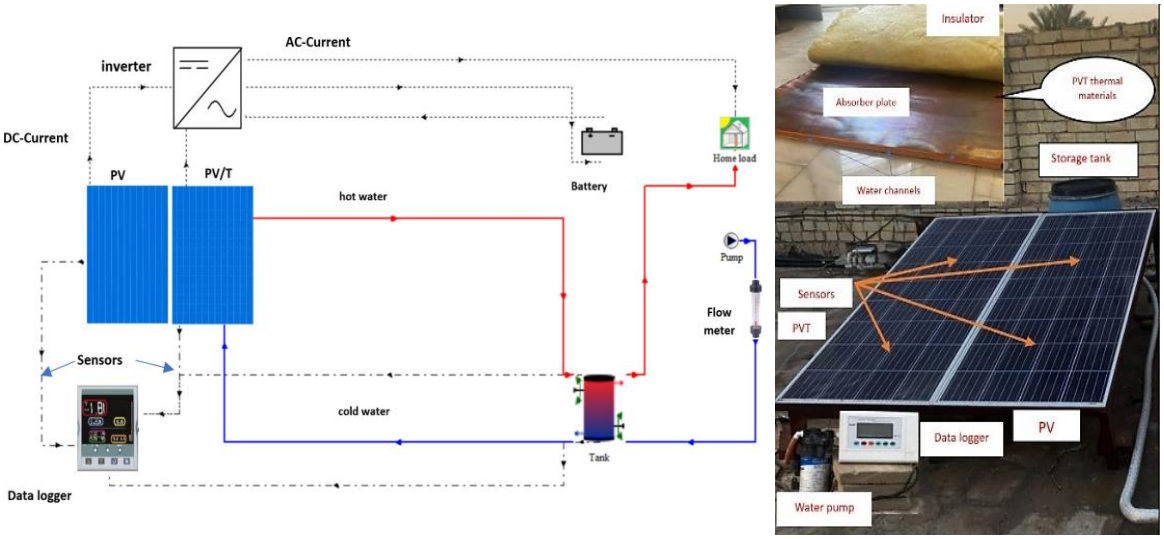

(a) (b)

Figure 1. Experimental setup: (a) general experimental schematic and (b) real installation setup

Table 1. PV/T materials description

Parameter	Description	Dimensions	units
Glass	low-iron glass	1.48×0.7×0.0032	m
PV	poly-crystalline	1.48×0.7×0.0003	m
Output power	160		w
Electrical efficiency	15.8		%
Solar cells no.	36		
Absorber plate	copper	1.46×0.69×0.0007	m
Channels rows	14 channels of copper	1.46×0.05×0.01	m
SCB	copper	r=0.004	m
Insulation	glass wool	1.48×0.7×0.3	m

2.2. Geometrical configuration

The proposed geometry includes fourteen rectangular channels or risers attached to the absorber plate, which is fixed at the PV panel backside by mechanical tools. Each one of these risers has 12 rows of SCB, and the attack angle is 30°. Generally, the performance of baffles or vortex generators depends on their installation, shapes, and numbers [30]. The proposed baffles were designed and installed taking into account the important

factors that were investigated in the previous studies. The physical model's component parts were all created using Solidworks software. The geometric design of the PV panel and the absorber plate with pipes (without baffles) have the same characteristics as the real ones used in this work's experimental setup. The whole geometry design and side view of one riser, as well as the ISO section for a part between two pairs of SCB, are illustrated in Figures 2(a)-2(c), respectively. Table 2 illustrates some of the used materials' physical properties.

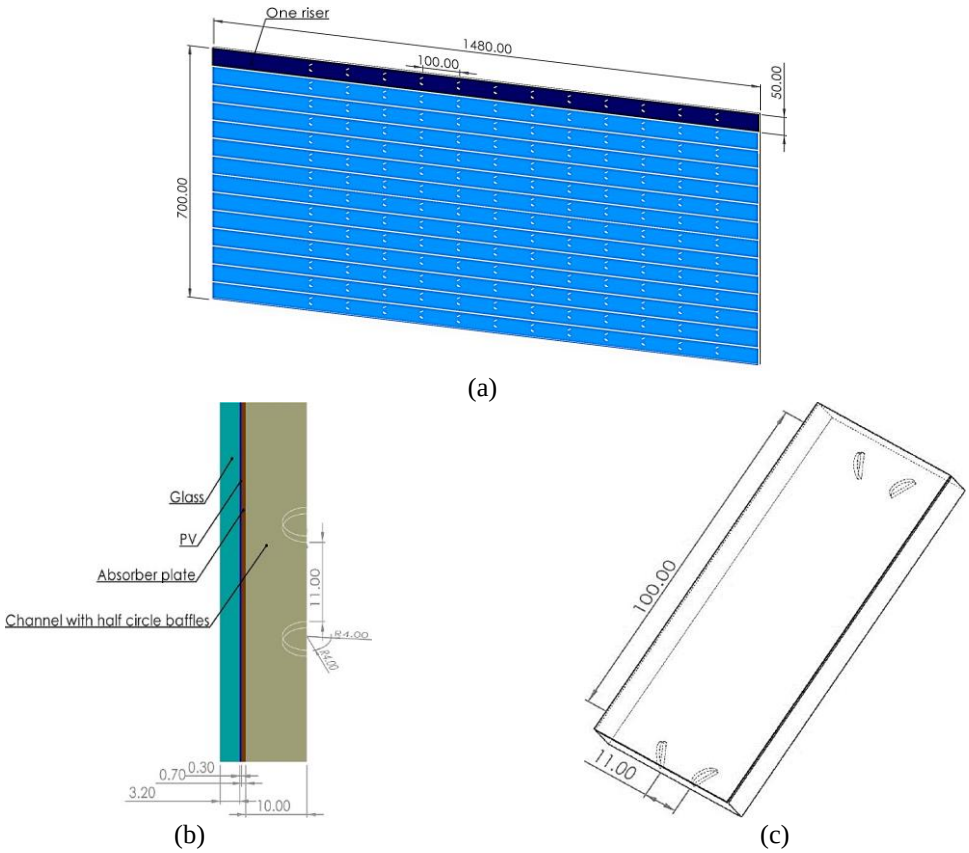

Figure 2. Geometry design: (a) whole geometry, (b) side view of one riser, and (c) ISO section of one riser

Table 2. Materials used properties

Materials	Thermal conductivity w/m.k	Density kg/m3	Specific heat capacity j/kg.k
Glass	1	2450	500
PV	148	2330	700
Copper	400	8940	385
Water	0.6	1000	4182

2.3. Mathematical model

2.3.1. Solver and governing equations

Basically, the fluid flow properties are based on Navier-Stockes equations (momentum equations), continuity, and energy equations. These equations can be expressed as (1)-(3).

$$\frac{\partial(\rho u_j)}{\partial x_j} \quad (1)$$

$$\frac{(\partial \rho u_i u_j)}{\partial x_j} = -\frac{\partial P}{\partial x_i} + \frac{\partial}{\partial x_j}\mu\left[\left(\frac{\partial u_i}{\partial x_j} + \frac{\partial u_j}{\partial x_i}\right)\right] \quad (2)$$

$$\frac{(\partial \rho u_i u_j)}{\partial x_j} = \frac{\partial}{\partial x_j}k\left[\left(\frac{\partial T}{\partial x_j}\right)\right] \quad (3)$$

The flow within the collector remains laminar at low speeds, characterized by a Reynolds number below 2300. However, the presence of baffles or vortex generators causes a transition to turbulent flow behavior [31].

Consequently, the solver model chosen for simulating the turbulent flow is the $k-\omega-SST$ (shear stress transport) model. The model introduced by Menter [32] is a combination of the $k-\epsilon$ [33] and $k-\omega$ [34] models. It is designed to provide accurate predictions for both the free stream and boundary layers of the flow. The mathematical expressions representing this model can be stated as (4) and (5):

$$\frac{D(\rho k)}{\partial t}=\frac{\partial}{\partial x_j}\left[(\mu+\mu_T\rho_k)\frac{\partial k}{\partial x_j}\right]+P_k-\rho\beta^*k\omega \tag{4}$$

$$\frac{D(\rho \omega)}{\partial t}=\frac{\partial}{\partial x_j}\left[(\mu+\mu_T\rho_\omega)\frac{\partial \omega}{\partial x_j}\right]+P_\omega-\rho\beta\omega^2+2(1-F_1)\rho\sigma_{\omega 2}\frac{1}{\omega}\frac{\partial k}{\partial x_i}\frac{\partial \omega}{\partial x_i} \tag{5}$$

$P_k=\tau_{ij}\frac{\partial u_i}{\partial x_j}, P_\omega=\gamma\frac{P_k}{\nu_T}$, where: $\tau_{ij}=2\mu_T\left(S_{ij}-\frac{1}{3}S_{kk}\delta_{ij}\right)-\frac{2}{3}\rho k\delta_{ij}, \gamma=\frac{\beta}{\beta^*}-\frac{k^2}{\sigma_\omega\sqrt{\beta^*}}$

where: $k=0.41, \beta^*=0.09$

$$\nu_T=\mu_T/\rho=a_1k/\max(a_1\omega, SF_2)$$
$$a_1=0.31, S=\sqrt{2S_{ij}S_{ij}}$$

$$F_1=\tanh(\xi^4), \xi=\min\left[\max\left\{\frac{\sqrt{k}}{\beta^*\omega y}, \frac{500\nu}{\omega y^2}\right\}, \frac{4\sigma\omega 2k}{CD_\omega y^2}\right]$$

$$CD_\omega=\max\left(\frac{2\sigma\omega 2}{\omega}\frac{\partial k}{\partial x_i}\frac{\partial \omega}{\partial x_i}, 10^{-10}S^{-2}\right)$$

$$F_2=\tanh\left[\left\{\max\left(\frac{2\sqrt{k}}{\beta^*y\omega}, \frac{500\nu}{\omega y^2}\right), \right\}^2\right]$$

$$(\sigma_k\sigma_\omega\beta)^T=F_1(\sigma_k\sigma_\omega\beta)_1^T+(1-F_1(\sigma_k\sigma_\omega\beta)_2^T)$$

$$\sigma_{k1}=0.85, \sigma_{k2}=1, \sigma_{\omega 1}=0.5, \sigma_{\omega 2}=0.856$$

Convection heat transfer coefficient (h), is calculated as (6).

$$h=\frac{q}{T_w-T_b} \tag{6}$$

Where, T_w and T_b are: wall and bulk temperature respectively. Bulk temperature is calculated from the (7) [35].

$$T_b=\frac{\iint_A v_nTdA}{\iint_A v_ndA} \tag{7}$$

Where, v_n : is the velocity component. The heat transfer rate can be expressed as (8).

$$q=m\cdot C_p(T_o-T_i) \tag{8}$$

The local Nusselt number is calculated from the (9).

$$Nu=\frac{hD}{k} \tag{9}$$

Where D is the hydraulic diameter and can be expressed as (10).

$$D_h=\frac{2ab}{a+b} \tag{10}$$

Nusselt number for the smooth channel can be written as (11) [36].

$$Nu_0 = 0.023Re^{0.8}\mathrm{Pr}^{0.8} \quad (11)$$

The friction factor can be calculated as (12).

$$f = \frac{2}{L\backslash D}\frac{\Delta p}{\rho U^2} \quad (12)$$

Electrical efficiency can be calculated according to the (13) [37].

$$\eta_{el} = \eta_{\mathrm{ref}} - \mu\left(T_{pv} - T_{ref}\right) \quad (13)$$

Where, the (14) and (15).

$$T_{pv} = T_i + Q_{th}k \quad (14)$$

$$k = \frac{1-F_R}{F_R U_L} \quad (15)$$

F_R and U_L are: heat removal factor and heat loss coefficient respectively. The thermal efficiency of the PV/T can be calculated from the (16).

$$\eta = \frac{m \cdot C_p(T_o - T_i)}{GA} \quad (16)$$

Where, G: is the radiation applied on the collector surface, A: is the collector's surface area. The cost-benefit ratio can be expressed as (17) [38].

$$CBR = \frac{\%\Delta p}{\%Nu} \quad (17)$$

Where $\%\Delta p$: is the variation in pressure drop, and $\%Nu$ is the variation in the Nusselt number.

2.3.2. Grid independent

The proposed geometry was meshed using Ansys Fluent Meshing, which is computational fluid dynamics (CFD) software. Meshing processes and refining have been conducted and repeated until good mesh quality is obtained so that mesh orthogonality does not exceed 0.2. Boundary layers near the walls and boundaries close to the baffles have high sensitivity compared to other regions because of the velocity and temperature gradients. Consequently, a mesh of these regions was refined and meshed into a smaller size. Multi-sections and views for the mesh geometry are illustrated in Figures 3(a)-3(c). Different numbers of grids have been taken to verify the mesh independence or to be sure of the correctness of the solution, as shown in Figures 4(a) and 4(b). One riser of the system has been taken into consideration to complete the computational analyses so as to reduce the domain of the solution. The PV panel back sheet and ethylene vinyl acetate (EVA) layers were considered one layer, with the PV cell layer [39].

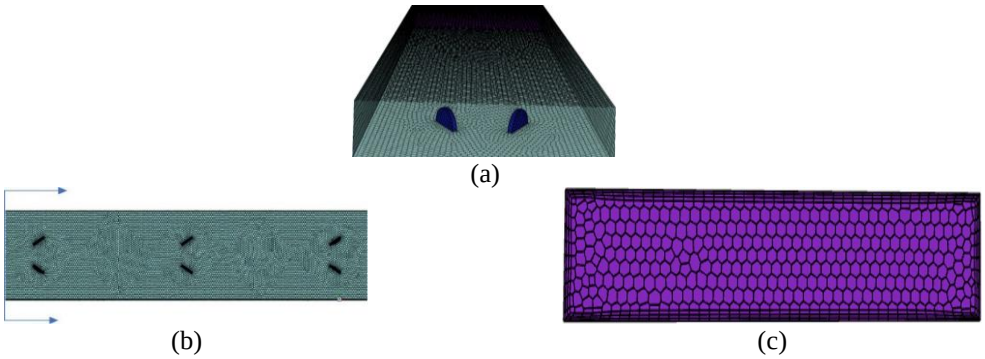

Figure 3. Geometry mesh of the riser: (a) ISO section, (b) top section view, and (c) front section view

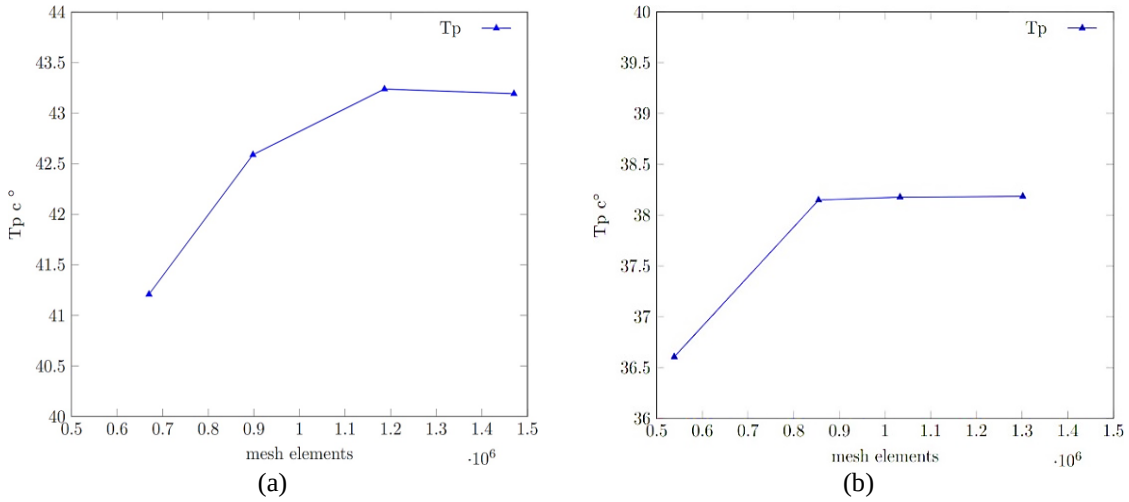

Figure 4. Mesh independent: (a) for the smooth channel and (b) for the channel with SCB

3. SOLVER, BOUNDARY CONDITIONS, AND VALIDATION

The present study's 3D-PV/T model runs under steady-state conditions; boundary conditions include fluid heat transfer for the solid domain and fluid dynamics for the fluid domain. The second-order upwind scheme was used to discretize the form of the momentum, energy, and pressure equations. This scheme couples the pressure and velocity without the need for a correction approach, unlike other schemes. The residuals of the momentum, energy, and continuity equations were $10^{-}6$, $10^{-}6$, and $10^{-}4$, respectively. Ansys mechanical software was employed to simulate the solid regions of the PV/T collector; furthermore, the fluid domain was simulated using fluent software; and finally, both simulations (fluid-solid) were combined through Ansys coupling system software to give the final result. The numerical solution operates under the following assumptions: i) Steady-state flow [40]; ii) PV-panel radiation and energy generation are neglected; and iii) Wind speed is uniform, and ambient temperature is constant during simulation.

The boundary conditions could be written as: on the top glass of the PV panels, solar irradiation and convection conditions were applied. The solar irradiation values are the same as in the experimental work. The bottom, left, and right sides of the riser are considered insulated. For the riser inlet, the mass flow rate condition was applied; in addition, the pressure outlet condition was set for the outlet boundary, which means the gradients of the variables at the outlet are zero. Validation was carried out by matching the numerical and experimental results. PV surface temperature was calculated for both cases, as well as water outlet temperature, and the results revealed a good match between experimental and numerical simulation results, as shown in Figures 5(a) and 5(b).

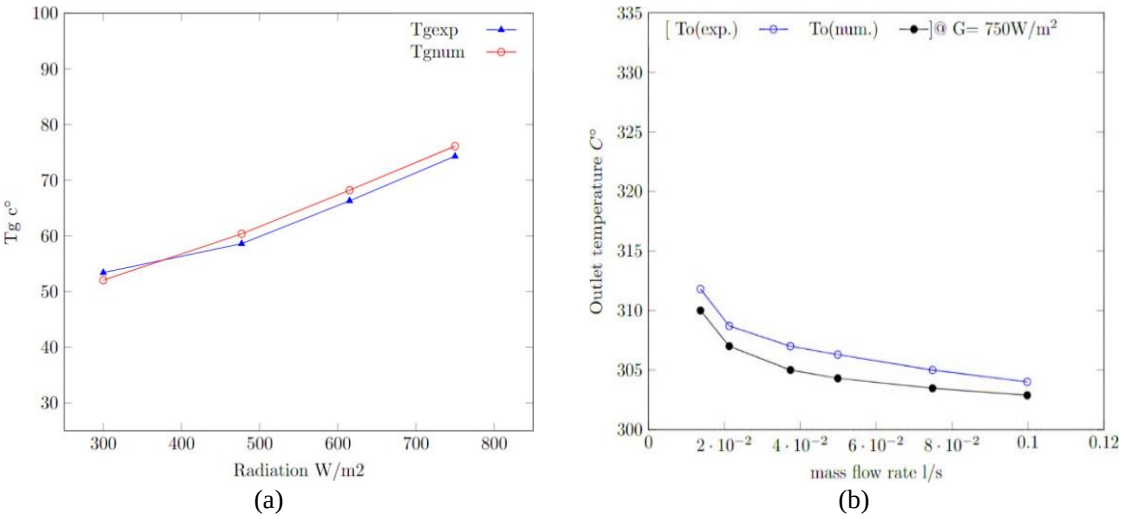

Figure 5. Results validation @ G = 750 W/m²: (a) glass temperature and (b) outlet fluid temperature

4. RESULTS AND DISCUSSION

4.1. Flow characteristic

As previously stated, baffles or vortex generators induce turbulence in the fluid flow, even when it is within the laminar zone. This flow pattern has a notable impact on improving heat transfer, particularly when there are additional factors that can increase the features of fluid flow, such as passive approaches that can transmit momentum or heat from the boundary to the main flow of the fluid. In turbulent flow, as mentioned, when the fluid approaches the boundary, a fast-moving swirling motion called an eddy or vortex interacts with the slower-moving fluid nearby. This interaction leads to an increase in speed and shear, as well as the formation of small-scale turbulence. The accelerated fluid is subsequently expelled from the boundary and directed away from it. Additionally, any obstacles encountered in the fluid stream can enhance turbulent diffusion and, consequently, promote fluid mixing. This is why turbulent flow is favored in numerous engineering applications [41]. In this study, it was observed that when the fluid comes into contact with the surface of the SCB, there is an immediate rise in the velocity of the fluid at the boundary layers. Additionally, the SCB effect increases thermal boundary layer mixing. In this manner, the high solid temperature will be transferred to the lower fluid temperature in order to achieve the desired outcome.

4.2. Nusselt number, friction factor, and cost-benefit ratio (CBR) effect

The Nusselt number is a metric used to assess the impact of convection on thermal conduction, and its criterion quantifies the extent to which heat transport can be augmented. In this study, the average Nusselt number has been determined for both smooth and enhanced channels using SCB. The results indicate that the presence of SCB has a significant impact on heat transfer rates. This is due to the restriction of fluid flow within the channel and the promotion of the boundary layer, which leads to better flow mixing and a boosted heat transfer rate. Figures 6(a) and 6(b) illustrate the impact of six different mass flow rates on the Nusselt number within the rectangular channel. By increasing the mass flow rate, the average Nusselt number increased in both cases (smooth and enhanced channels); however, compared to the smooth channel, the enhanced channel exhibited higher values. The values were (132.18, 89.52, 66.30, 57.11, 43.28, and 31.57) % for mass flow rates of (0.099, 0.074, 0.04, 0.037, 0.02, and 0.01) l/s, respectively. When conducting an analysis of the thermal performance of the system, it is crucial to understand the friction factor behavior and the impact of the pressure decrease.

Figures 7(a) and 7(b) illustrate the friction factor and pressure difference of the smooth and enhanced channels. It is obvious that the pressure difference of the enhanced channel is greater than that of the smooth channel due to the SCB series' effect, which creates a weak zone with low pressure behind it and a high-pressure zone in front of it. Consequently, the friction factor will be higher in the enhanced channel, as illustrated in the aforementioned figure. It is worth noting that the friction factor is not affected by the magnitude of radiation, as evidenced by the absence of a term in the equation that would cause radiation to affect the friction factor. The friction factor of the enhanced channel increased by (95.7, 74.6, 57.44, 46.68, 32.1, and 21.93) %, respectively, compared to that of the smooth channel, at Re = 4000, 3000, 200, 1500, 800, and 500. CBR is a metric that indicates the cost-effectiveness of the enhancement technique employed. The minimum value of CBR indicates that one is more efficient in the cost-benefit analysis, and the contrary is also true. The results indicated that the enhanced channel had a better CBR than the smooth channel. The enhanced one had an average CBR of 2.49, while the smooth one had an average CBR of 2.75. Consequently, pressure drops do not adversely affect the thermal performance.

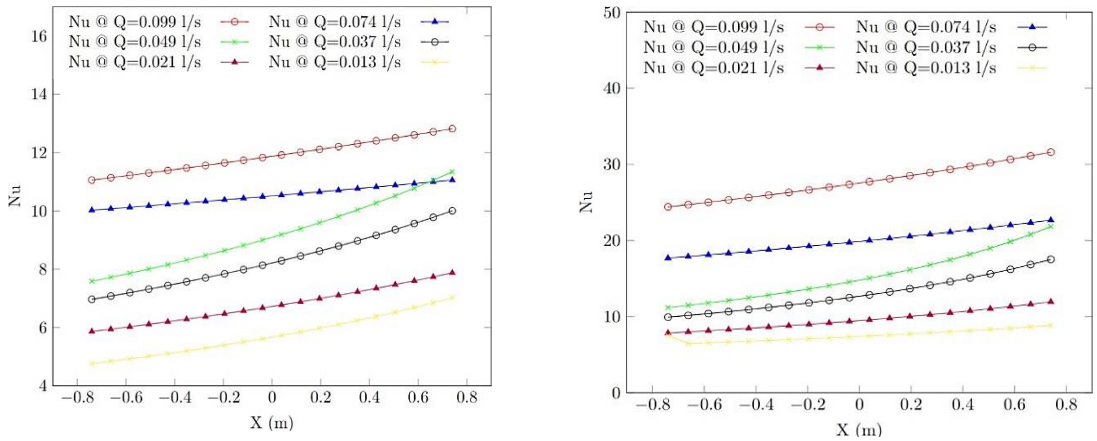

Figure 6. Nusselt number at different flow rate: (a) for the smooth channel and (b) for the enhanced channel

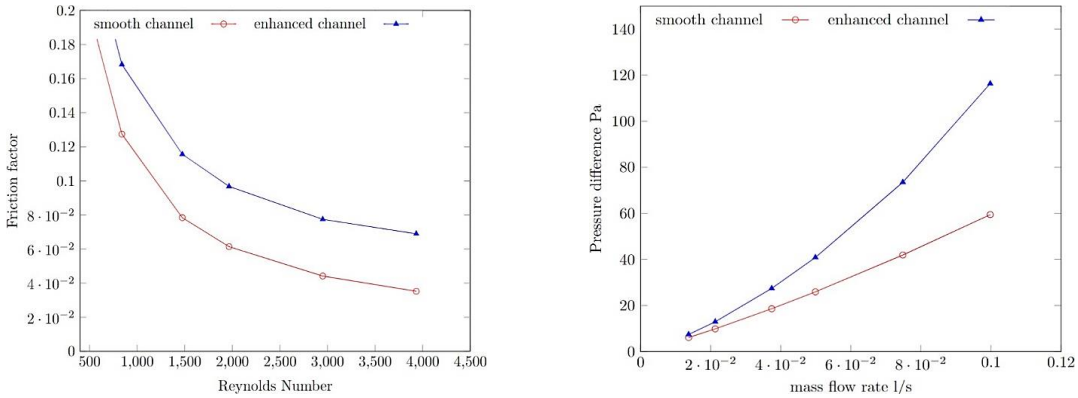

(a) (b)

Figure 7. Friction factor and pressure difference: (a) friction factor for the smooth and enhanced channels at different Re and (b) pressure drop for the smooth and enhanced channels

4.3. Thermal efficiency

PV/T collector thermal efficiency can be defined as the ratio of the thermal energy system rate to the dropped solar radiation. The thermal efficiency of the PV panel depends on the level of radiation and the collector's capacity to extract and transmit heat from the panel's surface to the fluid. Tables 3 and 4 display the computed thermal efficiency of the collector at various levels of radiation and mass flow rates. From the tables provided, it is obvious that increasing the mass flow rate leads to an increase in thermal efficiency for both the smooth and enhanced channels, regardless of the radiation magnitudes, until it reaches its maximum value. The enhanced channel exhibits better thermal efficiency compared to the smooth channel across different levels of radiation and mass flow rate. For instance, when the mass flow rate reaches its maximum, the thermal efficiency of the enhanced channel is (16.34, 18.83, 18.85, and 45.7) % higher than that of the smooth channel at G = (750, 615, 477, 300) W/m^2, respectively. Similarly, at the minimum mass flow rate, the thermal efficiency of the enhanced channel was (25.83, 19.27, 19.64, and 79.29) % higher than that of the smooth channel at G = (750, 615, 477, 300) W/m^2, respectively.

Table 3. PVT with smooth channel- efficiency

Radiation W/m^2	Mass flow rate L/s	Efficiency %	Radiation W/m^2	Mass flow rate L/s	Efficiency %
G = 750			G = 615		
	0.0998	21.55		0.0998	22.2
	0.07485	19.43		0.07485	20.24
	0.0499	16.05		0.0499	16.7
	0.037425	14.07		0.037425	14.62
	0.021307	11		0.021307	12.1
G = 477	0.013723	9.15	G = 300	0.021307	10.48
	0.0998	23.75		0.0998	30.42
	0.07485	21.77		0.07485	30.51
	0.0499	17.92		0.0499	26.78
	0.037425	16.8		0.037425	23.16
	0.021307	13.72		0.021307	17.65
	0.013723	11.21		0.021307	14.39

Table 4. PVT with enhanced channel efficiency

Radiation W/m^2	Mass flow rate L/s	Efficiency %	Radiation W/m^2	Mass flow rate L/s	Efficiency %
G = 750			G = 615		
	0.0998	25.71		0.0998	27.362
	0.07485	22.69		0.07485	23.81
	0.0499	19.21		0.0499	20
	0.037425	17.13		0.037425	17.78
	0.021307	13.42		0.021307	14.81
G = 477	0.013723	11.55	G = 300	0.021307	12.58
	0.0998	29.2		0.0998	56.08
	0.07485	25.63		0.07485	48.81
	0.0499	21.45		0.0499	41.02
	0.037425	19		0.037425	36.45
	0.021307	16.86		0.021307	30.36
	0.013723	13.47		0.021307	25.8

4.4. Electrical efficiency

As stated in the literature, higher temperatures of PV cells have a detrimental impact on both the output power and electrical efficiency. The manufacturer assigns a temperature coefficient factor to each solar panel. In this study, the PV panel being used has a temperature coefficient of 0.35°. This means that for every one degree increase in temperature above the standard test temperature, the electrical efficiency of the panel decreases by 0.35%. As a result, it is important to keep the PV panel temperature as close to the standard as possible in order to prevent more power losses. This matter is considered significant, particularly in areas with high radiation levels and hot climate conditions, as the temperature rises in relation to the intensity of radiation. Figures 8(a) and 8(b) illustrate the impact of the smooth and enhanced channels on the cooling effect of a PV system at various radiation and mass flow rate levels. The obtained temperature reduction for both cases was estimated by (4-20), and clearly, the optimum value was for the enhanced channel at the maximum value of the mass flow rate. Due to the cooling effect of the PV panel, the electrical efficiency of the panel rises as the mass flow rate increases. This improvement in electrical efficiency is observed at different radiation levels, with an increase of up to 32% for the smooth channels and up to 49% for the enhanced channels, as displayed in Figures 9(a) and 9(b).

4.5. Pressure drop, temperature, and velocity contours

Figures 10(a)-10(c) illustrate the contours of the pressure drop, temperature, and velocity at G = 750 W/m^2. In this figure, it is obvious that the pressure contour of the enhanced channel decreases rapidly in comparison to the smooth channel due to the restriction force generated by the SCB. This force forces the fluid to interface with the viscous and buffer sublayers, thereby increasing mixing and enhancing the rate of heat transfer. There are two categories of pressure drops: the first one occurs in the X-direction due to the heat flux effect, while the second occurs in the Y-direction due to the baffles or vorticity makers effect. Both types of pressure drops are present in the current study. To prevent a high decrease in electrical efficiency, it is crucial to keep PV panels at or near their standard operating temperature. Enhancing heat transfer within channels involves extracting an excessive amount of heat from the photovoltaic panels. The temperature contours illustrate the fluid's behavior within the channel in both cases. The temperature distribution in the enhanced channel is significantly better than that in the smooth channel. This enhancement results in a higher rate of heat transfer between the PV layers and the rectangular channel through the interface where the fluid and solid components meet. The velocity contours illustrate the fluid velocity trends, demonstrating an increase in velocity alongside and above the SCB while a decrease occurs behind it. This generates a secondary flow, which promotes effective mixing, reduces the thickness of the boundary layer, and thereby enhances the system's thermal efficiency. Table 5 displays the factors that were investigated in earlier studies, in addition to the ones explored in the current study.

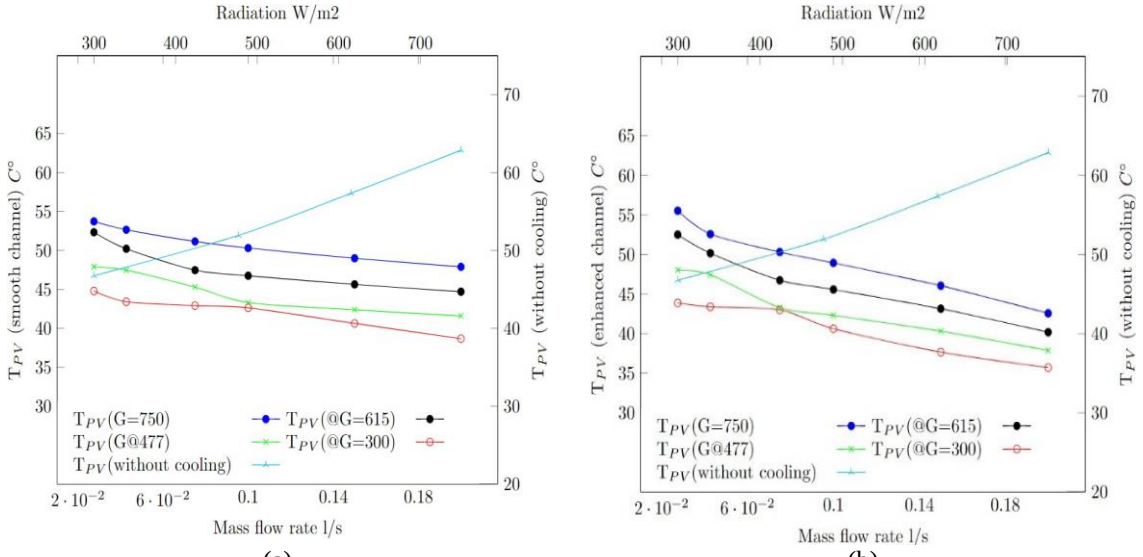

Figure 8. PV temperature at various flow rate magnitudes: (a) for the smooth channel and (b) for the enhanced channel

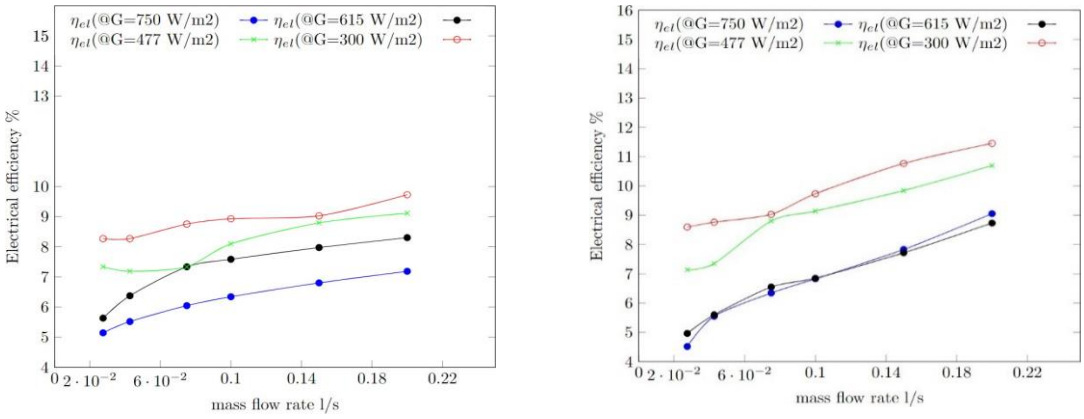

Figure 9. Electrical efficiency for various flow rate magnitudes: (a) for the smooth channel and (b) for the enhanced channel

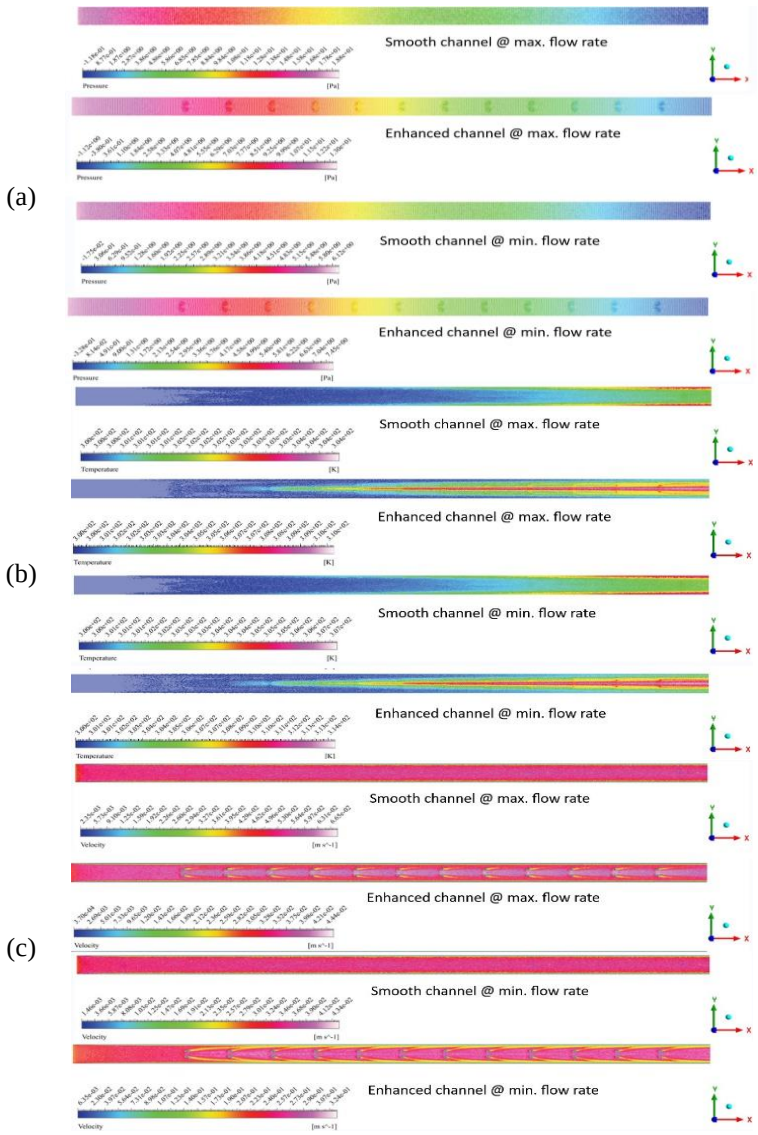

Figure 10. Contours of the flow characteristic at G =750 W/m^2 and maximum/minimum mass flow rate for the smooth and enhanced channels, respectively: (a) pressure distribution, (b) temperature distribution, and (c) velocity distribution

Table 5. Previous studies

No.	PV/T based technique	PV temperature reduction ◦C	Thermal efficiency increase%	Ref.
1	Vortex generator-free convection	2-3	-	[27]
2	Conical-leaf insert inside tube	up to 7	10.2-14.1	[26]
3	Cooling rectangular fin array	0.8-5.35	28.1–56.19	[42]
4	Wavy strip inside tube	4.59-14.62	6.92–8.64]	[43]
5	PCM inside channel	3.7–4.3.	-	[44]
6	Using structure of rack	up to 6.3	-	[45]
7	Heat sink	up to 10	-	[46]
8	Nanofluid with baffles	9.22-13.82	19.65-29.82	[47]
9	Water baffles	4-20	16.34 -79.29	Present study

5. CONCLUSION

The current study involves a numerical investigation of a water-based PV/T system using a multi-row SCB. The Nusselt number, friction factor, and thermal and electrical efficiency were computed and analyzed. Additionally, the pressure drop, velocity, and temperature contours were explained and discussed. PV cooling technology is essential for enhancing thermal efficiency, lowering operating temperatures, and consequently increasing electrical efficiency. Additionally, this technology enables the production of warm air or water that may be utilized in various applications. In summary, the conclusions can be briefly described as: i) A photovoltaic/thermal (PV/T) system is regarded as the optimal choice for minimizing energy losses and enhancing system efficiency; ii) The Nusselt number for the enhanced channel at a flow rate of 0.0998 l/s was more than 132% higher than that of the smooth channel. Similarly, the friction factor for the enhanced channel at a Reynolds number of 4000 was more than 95% higher than that of the smooth channel; iii) Compared to the smooth channel, the PV/T collector's thermal efficiency increased by about 16.34% to 79.29% when using SCB; iv) The electrical efficiency increased by about 32% and 49% for the smooth and enhanced channels, respectively; v) The smooth and enhanced channel resulted in a decrease in PV temperature of (4 to 20) °C; and vi) The average CBR for the enhanced channel was better than the smooth one.

REFERENCES

[1] Y. J. Sohn *et al.*, "Chemoautotroph Cupriavidus necator as a potential game-changer for global warming and plastic waste problem: A review," *Bioresource Technology*, vol. 340, p. 125693, Nov. 2021, doi: 10.1016/j.biortech.2021.125693.

[2] United Nations, *The Sustainable Development Goals Report 2022*, New York, 2022. [Online] Available: https://unstats.un.org/sdgs/report/2022/The-Sustainable-Development-Goals-Report-2022.pdf

[3] A. K. Digalwar and G. Giridhar, "Interpretive Structural modeling approach for development of Electric Vehicle market in India," *Procedia CIRP*, vol. 26, pp. 40–45, 2015, doi: 10.1016/j.procir.2014.07.125.

[4] M. Patil, A. Sidramappa, S. K. Shetty, and A. M. Hebbale, "Experimental study of solar PV/T panel to increase the energy conversion efficiency by air cooling," *Materials Today: Proceedings*, vol. 92, pp. 309–313, 2023, doi: 10.1016/j.matpr.2023.05.007.

[5] L. Gao, X. Zhang, and W. Hua, "Recent progress in photovoltaic thermal phase change material technology: A review," *Journal of Energy Storage*, vol. 65, 2023, doi: 10.1016/j.est.2023.107317.

[6] P. Dwivedi, K. Sudhakar, A. Soni, E. Solomin, and I. Kirpichnikova, "Advanced cooling techniques of P.V. modules: A state of art," *Case Studies in Thermal Engineering*, vol. 21, 2020, doi: 10.1016/j.csite.2020.100674.

[7] H. Ramdani and C. Ould-Lahoucine, "Study on the overall energy and exergy performances of a novel water-based hybrid photovoltaic-thermal solar collector," *Energy Conversion and Management*, vol. 222, 2020, doi: 10.1016/j.enconman.2020.113238.

[8] S. Odeh and M. Behnia, "Improving photovoltaic module efficiency using water cooling," *Heat Transfer Engineering*, vol. 30, no. 6, pp. 499–505, 2009, doi: 10.1080/01457630802529214.

[9] M. Wolf, "Performance analyses of combined heating and photovoltaic power systems for residences," *Energy Conversion*, vol. 16, no. 1–2, pp. 79–90, 1976, doi: 10.1016/0013-7480(76)90018-8.

[10] T. M. Sathe and A. S. Dhoble, "A review on recent advancements in photovoltaic thermal techniques," *Renewable and Sustainable Energy Reviews*, vol. 76, pp. 645–672, 2017, doi: 10.1016/j.rser.2017.03.075.

[11] H. Karkaba *et al.*, "Effect of using multiple vortex generator rows on heat transfer enhancement inside an asymmetrically heated rectangular channel," *Applied Thermal Engineering*, vol. 227, 2023, doi: 10.1016/j.applthermaleng.2023.120359.

[12] P. Rani and P. P. Tripathy, "Experimental investigation on heat transfer performance of solar collector with baffles and semicircular loops fins under varied air mass flow rates," *International Journal of Thermal Sciences*, vol. 178, 2022, doi: 10.1016/j.ijthermalsci.2022.107597.

[13] A. Hobbi and K. Siddiqui, "Experimental study on the effect of heat transfer enhancement devices in flat-plate solar collectors," *International Journal of Heat and Mass Transfer*, vol. 52, no. 19–20, pp. 4650–4658, 2009, doi: 10.1016/j.ijheatmasstransfer.2009.03.018.

[14] R. Kumar *et al.*, "Heat transfer and friction factor correlations for an impinging air jets solar thermal collector with arc ribs on an absorber plate," *Sustainable Energy Technologies and Assessments*, vol. 47, 2021, doi: 10.1016/j.seta.2021.101523.

[15] M. H. Alkhafaji, B. Freegah, and M. H. Alhamdo, "Study the influence of adding fins to the plate of the solar collector on thermal performance under natural phenomena," *International Communications in Heat and Mass Transfer*, vol. 135, 2022, doi: 10.1016/j.icheatmasstransfer.2022.106058.

[16] L. S. Sundar, A. H. Misganaw, M. K. Singh, A. M. B. Pereira, and A. C. M. Sousa, "Efficiency, energy and economic analysis of twisted tape inserts in a thermosyphon solar flat plate collector with Cu nanofluids," *Renewable Energy Focus* , vol. 35, pp. 10–31, 2020, doi: 10.1016/j.ref.2020.06.004.

[17] Y. Fu *et al.*, "A novel structure design and numerical analysis of porous media-assisted enhanced thermal performance of flat-plate solar collector," *Thermal Science and Engineering Progress*, vol. 40, 2023, doi: 10.1016/j.tsep.2023.101777.

[18] S. Algarni, "Evaluation and optimization of the performance and efficiency of a hybrid flat plate solar collector integrated with phase change material and heat sink," *Case Studies in Thermal Engineering*, vol. 45, 2023, doi: 10.1016/j.csite.2023.102892.
[19] T. desisa Rago, "Experimental and Numerical Investigation of Heat Transfer Characteristics in Solar Flat Plate Collector Using Nanofluids," *SSRN Electronic Journal*, 2022, doi: 10.2139/ssrn.4282071.
[20] F. A. S. da Silva, D. J. Dezan, A. V. Pantaleão, and L. O. Salviano, "Longitudinal vortex generator applied to heat transfer enhancement of a flat plate solar water heater," *Applied Thermal Engineering*, vol. 158, 2019, doi: 10.1016/j.applthermaleng.2019.113790.
[21] S. S. M. Ajarostaghi, M. Zaboli, H. Javadi, B. Badenes, and J. F. Urchueguia, "A Review of Recent Passive Heat Transfer Enhancement Methods," *Energies*, vol. 15, no. 3, 2022, doi: 10.3390/en15030986.
[22] G. Zhou and Q. Ye, "Experimental investigations of thermal and flow characteristics of curved trapezoidal winglet type vortex generators," *Applied Thermal Engineering*, vol. 37, pp. 241–248, 2012, doi: 10.1016/j.applthermaleng.2011.11.024.
[23] A. Kumar and B. Prasad, "Investigation of twisted tape inserted solar water heaters—heat transfer, friction factor and thermal performance results," *Renewable Energy*, vol. 19, no. 3, pp. 379–398, 2000.
[24] J. Wang and Y. Zhao, "Heat and fluid flow characteristics of a rectangular channel with a small diameter circular cylinder as vortex generator," *International Journal of Thermal Sciences*, vol. 92, pp. 1–13, 2015, doi: 10.1016/j.ijthermalsci.2015.01.018.
[25] A. T. Wijayanta, T. Istanto, K. Kariya, and A. Miyara, "Heat transfer enhancement of internal flow by inserting punched delta winglet vortex generators with various attack angles," *Experimental Thermal and Fluid Science*, vol. 87, pp. 141–148, 2017, doi: 10.1016/j.expthermflusci.2017.05.002.
[26] S. R. Maadi, H. Sabzali, A. Kolahan, and D. Wood, "Improving the performance of PV/T systems by using conical-leaf inserts in the coolant tubes," *Solar Energy*, vol. 212, pp. 84–100, 2020, doi: 10.1016/j.solener.2020.10.011.
[27] Z. Zhou *et al.*, "Passive PV module cooling under free convection through vortex generators," *Renewable Energy*, vol. 190, pp. 319–329, 2022, doi: 10.1016/j.renene.2022.03.133.
[28] N. Kaewchoothong, T. Sukato, P. Narato, and C. Nuntadusit, "Flow and heat transfer characteristics on thermal performance inside the parallel flow channel with alternative ribs based on photovoltaic/thermal (PV/T) system," *Applied Thermal Engineering*, vol. 185, 2021, doi: 10.1016/j.applthermaleng.2020.116237.
[29] F. Yazdanifard, E. Ebrahimnia-Bajestan, and M. Ameri, "Investigating the performance of a water-based photovoltaic/thermal (PV/T) collector in laminar and turbulent flow regime," *Renewable Energy*, vol. 99, pp. 295–306, 2016, doi: 10.1016/j.renene.2016.07.004.
[30] Y. Amini and S. E. Habibi, "Effects of multiple flexible vortex generators on the hydrothermal characteristics of a rectangular channel," *International Journal of Thermal Sciences*, vol. 175, 2022, doi: 10.1016/j.ijthermalsci.2021.107454.
[31] A. J. Larki, A. Ghafouri, E. Assareh, and M. Moravej, "Numerical investigation of the influence of a rotating vortex generator array on the performance of a thermal storage system," *Journal of Building Engineering*, vol. 55, 2022, doi: 10.1016/j.jobe.2022.104640.
[32] F. R. Menter, "Two-Equation Eddy-Viscosity Turbulence Models for Engineering Applications," *AIAA Journal*, vol. 32, no. 8, pp. 1598–1605, 1994.
[33] W. P. Jones and B. E. Launder, "The prediction of laminarization with a two-equation model of turbulence," *International Journal of Heat and Mass Transfer*, vol. 15, no. 2, pp. 301–314, Feb. 1972, doi: 10.1016/0017-9310(72)90076-2.
[34] D. C. Wilcox, "Turbulence Modelling for CFD 3rd Edition," in *Turbulence Modeling for CFD*, 1993, p. 536.
[35] I. Tosun, "Modeling in Transport Phenomena: A Conceptual Approach," in *Modeling in Transport Phenomena: A Conceptual Approach*, 2007, pp. 1–606.
[36] B. Sundén, *Introduction to heat transfer*. UK: Wit Press, 2012.
[37] S. Dubey, J. N. Sarvaiya, and B. Seshadri, "Temperature Dependent Photovoltaic (PV) Efficiency and Its Effect on PV Production in the World – A Review," *Energy Procedia*, vol. 33, pp. 311–321, 2013, doi: 10.1016/j.egypro.2013.05.072.
[38] O. Heriyani, M. Djaeni, Syaiful, and A. K. Putri, "Perforated concave rectangular winglet pair vortex generators enhance the heat transfer of air flowing through heated tubes inside a channel," *Results in Engineering*, vol. 16, 2022, doi: 10.1016/j.rineng.2022.100705.
[39] A. Zabihi Sheshpoli, O. Jahanian, K. Nikzadfar, and M. Aghajani Delavar, "Numerical and experimental investigation on the performance of hybrid PV/thermal systems in the north of Iran," *Solar Energy*, vol. 215, pp. 108–120, 2021, doi: 10.1016/j.solener.2020.12.036.
[40] S. D. Prasetyo, A. R. Prabowo, and Z. Arifin, "The use of a hybrid photovoltaic/thermal (PV/T) collector system as a sustainable energy-harvest instrument in urban technology," *Heliyon*, vol. 9, no. 2, 2023, doi: 10.1016/j.heliyon.2023.e13390.
[41] J. Southard, "Special Topics: An Introduction to Fluid Motions, Sediment Transport, and Current-generated Sedimentary Structures (Lecture Notes)," *Earth, Atmospheric, and Planetary Sciences*, pp. 184–200, 2006, [Online]. Available: http://ocw.mit.edu/courses/earth-atmospheric-and-planetary-sciences/12-090-special-topics-an-introduction-to-fluid-motions-sediment-transport-and-current-generated-sedimentary-structures-fall-2006/lecture-notes/%5Cnhttp://ocw.mit.edu/courses/earth-atmospher.
[42] J. C. Mojumder, W. T. Chong, H. C. Ong, K. Y. Leong, and Abdullah-Al-Mamoon, "An experimental investigation on performance analysis of air type photovoltaic thermal collector system integrated with cooling fins design," *Energy and Buildings*, vol. 130, pp. 272–285, 2016, doi: 10.1016/j.enbuild.2016.08.040.
[43] S. R. Maadi, A. Navegi, E. Solomin, H. S. Ahn, S. Wongwises, and O. Mahian, "Performance improvement of a photovoltaic-thermal system using a wavy-strip insert with and without nanofluid," *Energy*, vol. 234, 2021, doi: 10.1016/j.energy.2021.121190.
[44] N. Choubineh, H. Jannesari, and A. Kasaeian, "Experimental study of the effect of using phase change materials on the performance of an air-cooled photovoltaic system," *Renewable and Sustainable Energy Reviews*, vol. 101, pp. 103–111, 2019, doi: 10.1016/j.rser.2018.11.001.
[45] F. Al-Amri, F. Saeed, and M. A. Mujeebu, "Novel dual-function racking structure for passive cooling of solar PV panels –thermal performance analysis," *Renewable Energy*, vol. 198, pp. 100–113, 2022, doi: 10.1016/j.renene.2022.08.047.
[46] J. G. Hernandez-Perez, J. G. Carrillo, A. Bassam, M. Flota-Banuelos, and L. D. Patino-Lopez, "A new passive PV heatsink design to reduce efficiency losses: A computational and experimental evaluation," *Renewable Energy*, vol. 147, pp. 1209–1220, 2020, doi: 10.1016/j.renene.2019.09.088.
[47] M. Ahmadinejad and R. Moosavi, "Energy and exergy evaluation of a baffled-nanofluid-based photovoltaic thermal system (PVT)," *International Journal of Heat and Mass Transfer*, vol. 203, p. 123775, 2023, doi: 10.1016/j.ijheatmasstransfer.2022.123775.

BIOGRAPHIES OF AUTHORS

Hayder Altharwanee is a Ph.D. student in the Department of Electrical Engineering at the University of Jaén , Spain. He holds a master's degree in Energy Conversion from Ferdowsi University of Mashhad (FUM), Iran. Currently, his research focuses on renewable energy technologies, hybrid energy systems, photovoltaic thermal systems, heat transfer enhancement, etc. With a strong foundation in energy conversion, his objective is to make a meaningful contribution to the development of sustainable energy solutions and innovative technologies in the field of electrical and mechanical engineering. He can be contacted at email: hta00003@red.ujaen.es.

Francisco Jurado is a coordinator of the Electrical Engineering Department at the University of Jaén (UJA), Jaen, Spain. Francisco Jurado (Senior Member, IEEE) received the M.Sc. and Ph.D. degrees from Universidad Nacional de Educacio´n a Distancia (UNED), Madrid, Spain, in 1995 and 1999, respectively. He is currently a full professor with the Department of Electrical Engineering, University of Jaen, Spain. His research activities have been devoted to several topics, including power systems, and renewable energy. He is author of more than 500 papers in journals included in the Journal Citation Report (JCR), about 220 papers in the proceedings of international conferences, and 6 books. He has been involved in research projects funded by Spanish Ministries and European Commission. He is also the researcher among the most influential in the world according to the classification made by Stanford University (USA). He can be contacted at email: fjurado@ujaen.es.

David Vera got his Ph.D. in Industrial Engineer by the University of Jaén (since 2013). Currently, he is an associate professor in the same university in the area of Energy and Electrical Engineering. Previously, he worked in a private company (EnergyLab Technology Center) from 2013 to 2015. Regarding the research activity, his work is focused on renewable energy technologies, concretely in biomass gasification and combustion, distributed generation technologies and waste valorization. He has participated in several research projects. One of the most important was the participation in a European Project (RESOLIVE) funded by the 7th Framework Programme with 1.4 M€. Currently, He is the principal investigator and coordinator of an international project (ERANET-ARIMNet 2) called OLIVEN funded with 227.000 €. He can be contacted at email: dvera@ujaen.es.